PHENOMENOLOGICAL MODEL OF DEPTH MEMBRANE FILTRATION

Polyakov Yu.S.
USPolyResearch, USA; ypolyakov@uspolyresearch.com

The conventional approach to designing ultrafiltration/microfiltration (UF/MF) filters based on reduction of the concentration polarization and particle deposition to increase the permeate velocity is inherently associated with additional expenditures of power or other material resources, which makes it not enough cost-effective to be competitive with non-membrane filtration processes in water and wastewater treatment applications. A completely opposite process design strategy based on utilization of the particle deposition on membrane surface to produce an additional (to permeate) volume of clarified water was recently suggested [1]. The latter process, called depth membrane filtration, does not require additional power expenditures and can provide high water recoveries, implying its high cost-effectiveness. The process theory is based on the assumption that the decrease in the rate of cake deposition can be caused by the desorption of particles from the membrane, or cake, surface. That is why the deposition equation in Ref. [1] has the form of reversible adsorption. However, most of the experimental studies on the transport of colloidal particles indicate that the desorption of colloidal particles is hardly likely in most practical applications. It is therefore of interest to study the depth membrane filtration process without particle desorption in which the decline in the rate of cake deposition is caused by the decrease in deposition coefficient due to the effect of repulsive colloidal interactions, permeation drag decline, and the like, which is implied by the modern theory of depth filtration [2].

Consider a process of depth membrane filtration in which a dilute suspension with constant density and viscosity is clarified in a hollow fiber membrane (HFM) adsorber (Fig. 1). The vacuum providing a constant transmembrane pressure, which is the driving force of membrane filtration, is produced in the HFM lumens. The HFM packing density is close to the packing densities of granular beds, that is, about 0.5. Assume that the porous HFM membranes completely reject the suspended particles. The feed concentration and temperature remain constant. The diffusion of particles beyond the layer of surface forces is ignored, and the suspension is perfectly mixed in the plane

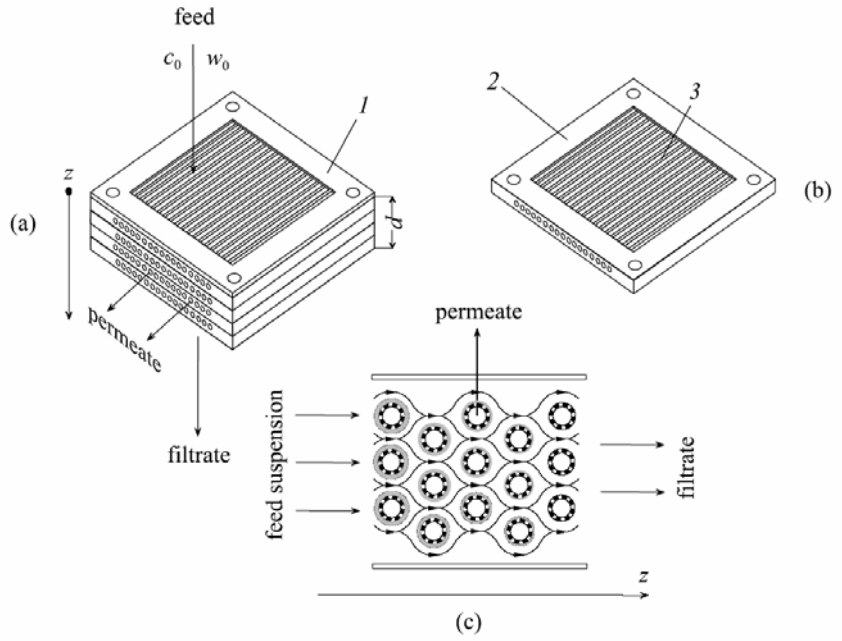

Fig. 1. Rectangular cartridge-type outside-in hollow fiber membrane filter:
(a) cartridge of HFM wafers (*1*, top plate; *d*, filter depth), (b) HFM wafer (*2*, perforated frame; *3*, hollow fiber membrane), and (c) flow diagram (gray solid rings – cake layers; porous rings – hollow fibers)

perpendicular to the flow of liquid across the filter due to local flow instabilities and interfiber vortices and eddies. Particle dispersion and effects of filter housing walls are assumed to be negligible. The differential law of mass conservation can then be written as

$$\frac{\partial c}{\partial t}+\frac{\partial (c w)}{\partial z}=-s\frac{\partial \Gamma}{\partial t}, \tag{1}$$

where c is the concentration of suspended particles; t, the time; z, the filter depth coordinate; the liquid velocity w is the velocity averaged over the cross section of all interfiber channels at z; $s=S_m/(S\,d)$, the ratio of HFM shell surface area to the suspension volume inside the filter; Γ, specific cake deposit (cake mass per square meter of HFM shell surface area), S_m, the total HFM shell surface area; S, the total cross section area of the interfiber space; *d*, the overall filter depth.

The permeate velocity of a hollow fiber membrane is governed by Darcy's law:

$$V_p=\frac{P}{\mu\,(R_m+r_c\,\Gamma)}, \tag{2}$$

where V_p is the permeate velocity; *P*, the transmembrane pressure (TMP); μ, the liquid viscosity; $R_m=P/(\mu\,V_0)$ is the clean membrane resistance; and r_c is the specific cake resistance.

Liquid continuity equation in integral form is written as

$$w=w_0-\int_0^z s\,V_p\,dz, \tag{3}$$

where w_0 is the constant feed velocity. This implies that the decline in permeate flow rate with time is compensated by the equal increase in filtrate flow rate.

It is also assumed that the formation of cake layer on the HFM shells cannot noticeably change the geometrical dimensions of interfiber channels, and that the value of TMP is the same throughout the channels.

A clean filter initial condition will be used. The suspension concentration at filter inlet is assumed to be constant:

$$c=c_0 \qquad \text{when } z=0,\ t>0; \tag{4}$$

$$c=0,\ \Gamma=0 \qquad \text{when } t=0,\ z>0. \tag{5}$$

To close the system of equations, a specific expression for the deposition rate in Eq. (1) has to be selected. In general, the deposition rate equation for an outside-in HFM filter, that is, for a depth filter with semipermeable particle collectors, may be written as

$$\frac{\partial \Gamma}{\partial t}=k_1(\psi,\Gamma)\,c-k_2\,\Gamma+k_3\,V_p\,c, \tag{6}$$

where k_1 is the deposition coefficient; ψ, the parameter vector characteristic of the filtration process; k_2, the re-entrainment coefficient; k_3 is a constant.

The first term on the right side of Eq. (6) is adopted from depth filtration theories [2], describing the deposition flux of particles onto the membrane surface (or onto the cake layer after it is formed). For Brownian (submicron) particles, the deposition is usually caused by Brownian diffusion and surface (colloidal) interaction forces, such as electrical double layer and van der Waals forces. For micron particles, the deposition is typically attributed to inertial impaction, interception, sedimentation, electrostatic forces, and surface interaction forces. In general, the deposition coefficient k_1 varies with specific cake deposit Γ, which takes into account the effect of deposited particles on the deposition flux.

The second term on the right side of Eq. (6) is adopted from depth filtration [2] and reversible adsorption theories, describing the particle detachment flux from the membrane

surface (or cake layer). For Brownian particles, the re-entrainment is usually caused by desorption of particles from the collector surface. For micron particles, the re-entrainment is commonly attributed to unfavorable hydrodynamic conditions (flow instabilities). Generally, the re-entrainment coefficient k_2 may be variable.

The last term in Eq. (6) accounts for the deposition rate increase due to the permeation drag. The linear dependence of the deposition rate on the product of permeate velocity and particle concentration is selected because the classical cake filtration equation, which corresponds to $k_1 = 0,\ k_2 = 0,\ k_3 = 1$, can describe the permeate flux decline in some surface microfiltration experiments without axial flow.

A number of studies showed that particle deposition on HF membranes is usually irreversible. Neglecting the particle detachment flux and using the fact that V_p is a function of Γ, Eq. (6) may be rewritten as

$$\frac{\partial \Gamma}{\partial t} = \beta(\boldsymbol{\psi}, \Gamma)\, c\,, \tag{7}$$

where β is a general function of Γ depending on the parameter vector characteristic of the filtration process $\boldsymbol{\psi}$, the components of which are phenomenological constants [2].

The problem (1)–(5), (7) with the help of simple mathematical transformations takes the following form for the function Γ:

$$\frac{\partial}{\partial t}\left(\frac{1}{\beta(\Gamma)}\frac{\partial \Gamma}{\partial t}\right) + \frac{\partial\left(\frac{1}{\beta(\Gamma)}\frac{\partial \Gamma}{\partial t}\left\{w_0 - sV_0\int_0^z \frac{dz}{1+\chi_1\Gamma}\right\}\right)}{\partial z} = -s\frac{\partial \Gamma}{\partial t}, \tag{8}$$

$$z = 0,\ t > 0: \quad \Gamma = \Gamma_0; \qquad t = 0,\ z > 0: \quad \Gamma = 0,\ \frac{\partial \Gamma}{\partial t} = 0; \tag{9}$$

where Γ_0 is found by solving the equation

$$\frac{d\Gamma_0}{dt} = \beta(\Gamma_0) c_0\,, \tag{10}$$

$$t = 0,\ \ \Gamma_0 = 0\,. \tag{11}$$

Here $\chi_1 = r_c / R_m$.

Converting the problem (8)–(9) into dimensionless form gives:

$$\frac{\partial}{\partial \tau}\left(\frac{1}{\mathrm{B}(\gamma)}\frac{\partial \gamma}{\partial \tau}\right) + \frac{1}{N_\beta}\frac{\partial}{\partial Z}\left(\frac{1}{\mathrm{B}(\gamma)}\frac{\partial \gamma}{\partial \tau}\left\{1 - \xi\int_0^Z \frac{dZ}{1+N_\chi\gamma}\right\}\right) = -\frac{\partial \gamma}{\partial \tau}, \tag{12}$$

$$Z = 0,\ \tau > 0: \quad \gamma = \gamma_0; \qquad \tau = 0,\ Z > 0: \quad \gamma = 0,\ \frac{\partial \gamma}{\partial \tau} = 0; \tag{13}$$

where $\tau = s\beta\, t,\ Z = \frac{z}{d},\ \gamma = \frac{s}{c_0}\Gamma,\ N_\chi = \chi_1\frac{c_0}{s},\ N_\beta = \frac{s\beta\, d}{w_0},\ N_\alpha = \frac{\alpha}{s\beta},\ \xi = \frac{sV_0\, d}{w_0}$.

Here γ_0 is found by solving

$$\frac{d\gamma_0}{d\tau} = \mathrm{B}(\gamma_0)\,, \tag{14}$$

$$\tau = 0,\ \ \gamma_0 = 0\,. \tag{15}$$

The two main functions to be found are the dimensionless permeate velocity averaged over the adsorber depth

$$V = \int_0^1 \frac{dZ}{1+N_\chi\gamma} \tag{16}$$

and the dimensionless concentration of suspended particles C_f at the filter outlet (filtrate concentration)

$$C_f = \frac{1}{\mathrm{B}\left[\gamma(\tau,1)\right]}\frac{\partial\gamma(\tau,1)}{\partial\tau}. \tag{17}$$

Introducing a new function

$$v = \int_0^Z \frac{dZ}{1+N_\chi\,\gamma}, \tag{18}$$

which represents the permeate flow rate for the filter region found between the adsorber inlet and the plane with coordinate Z, reduces the problem to solving the equation:

$$\frac{\partial}{\partial\tau}\left(\frac{1}{\mathrm{B}\left[\partial v/\partial Z\right]}\frac{\partial^2 v}{\partial Z\,\partial\tau}\left(\frac{\partial v}{\partial Z}\right)^{-2}\right)+\frac{1}{N_\beta}\frac{\partial}{\partial Z}\left(\frac{1}{\mathrm{B}\left[\partial v/\partial Z\right]}\frac{\partial^2 v}{\partial Z\,\partial\tau}\left(\frac{\partial v}{\partial Z}\right)^{-2}(1-\xi v)\right)=-\frac{\partial^2 v}{\partial Z\,\partial\tau}\left(\frac{\partial v}{\partial Z}\right)^{-2} \tag{19}$$

with initial and boundary conditions

$$v(0,Z)=Z,\ v(\tau,0)=0,\ \frac{\partial v(0,Z)}{\partial\tau}=0,\ \frac{\partial v(\tau,0)}{\partial Z}=\frac{1}{1+N_\chi\,\gamma(\tau,0)}. \tag{20}$$

Problem (19)–(20) can be solved numerically using the generalized implicit Crank-Nicholson finite difference method [3]. In this case, $V(\tau)=v(\tau,1)$ and the dimensionless specific cake deposit γ can be calculated from

$$\gamma=\frac{1}{N_\chi}\left[\left(\frac{\partial v}{\partial z}\right)^{-1}-1\right]. \tag{21}$$

As the filtrate concentration given by Eq. (17) and other particle retention characteristics of the filter are functions of partial derivatives of v with respect to time and coordinate, the latter should be calculated with a very high accuracy. Considering that Eq. (19) is a strongly nonlinear partial differential equation, the numerical solution would consume too much time to be used in practical calculations. Therefore, a much faster approximate solution is developed next.

The end-point interpolation method using the average value of permeate velocity [4] will be applied. With a constant value of $V_p=\langle V_p\rangle$, Eqs. (1)-(3) can be rewritten as

$$\frac{\partial c}{\partial t}+\left(w_0-s\langle V_p\rangle z\right)\frac{\partial c}{\partial z}=-s\frac{\partial\Gamma}{\partial t}+s\langle V_p\rangle c, \tag{22}$$

$$\langle V_p\rangle=\frac{1}{t\,d}\int_0^{t_1}\int_0^{d}\frac{1}{1+\chi_1\,\Gamma\left(t,z,\langle V_p\rangle\right)}dz_1\,dt_1. \tag{23}$$

Introducing a new coordinate $x=-\dfrac{w_0}{s\langle V_p\rangle}\ln\left[1-\dfrac{s\langle V_p\rangle}{w_0}z\right]$, Eq. (22) is transformed to

$$\frac{\partial c}{\partial t}+w_0\frac{\partial c}{\partial x}=-s\frac{\partial\Gamma}{\partial t}+s\langle V_p\rangle c. \tag{24}$$

The exact solution to the problem (24), (7), (4)-(5) in terms of uncoupled ordinary differential equations can be obtained using the technique described in Ref. [2]. The mass conservation principle applied to a layer of hollow fibers of corrected depth η over a time interval of 0 to T leads to

$$\int_0^T w_0 c_0\,dt=\int_0^T w_0\,c(\eta,t)\,dt+\int_0^{\eta}\left(s\Gamma(x,T)+c(x,T)-s\int_0^T c(x,t)\,\langle V_p\rangle\,dt\right)dx. \tag{25}$$

According to Eq. (7),

$$c(\eta,t)=\frac{1}{\beta(\Gamma)}\left.\frac{\partial\Gamma}{\partial t}\right|_\eta. \tag{26}$$

As Γ is a function of t and x, $d\Gamma$ can be written as

$$d\Gamma = \left(\frac{\partial \Gamma}{\partial t}\right)_x dt + \left(\frac{\partial \Gamma}{\partial x}\right)_t dx, \tag{27}$$

which at $x = \eta$ becomes

$$d\Gamma = \left(\frac{\partial \Gamma}{\partial t}\right)_\eta dt. \tag{28}$$

Substituting Eqs. (26)-(28) into Eq. (25), differentiating with respect to η, and replacing η and T with x and t, respectively, yields

$$\left(\frac{\partial \Gamma}{\partial x}\right)_t = -\frac{\beta(\Gamma)}{w_0}\left(s\Gamma + c - s\langle V_p\rangle \int_0^\Gamma \frac{d\Gamma}{\beta(\Gamma)} \right). \tag{29}$$

Introducing a new time coordinate $\theta = t - x/w_0$, one obtains

$$\left(\frac{\partial \Gamma}{\partial x}\right)_\theta = -\frac{s\beta(\Gamma)}{w_0}\left(\Gamma - \langle V_p\rangle \int_0^\Gamma \frac{d\Gamma}{\beta(\Gamma)} \right). \tag{30}$$

The exact solution to the problem (24), (7), (4)-(5) in dimensionless form can then be written as

$$\frac{d\gamma}{dX} = -\mathrm{B}(\gamma)\left(N_\beta \gamma - \xi_{av} \int_0^\gamma \frac{d\gamma}{\mathrm{B}(\gamma)} \right), \tag{31}$$

$$X = 0,\ \gamma = \gamma_0, \tag{32}$$

where $X = -\ln[1 - \xi_{av} Z]/\xi_{av}$, $\xi_{av} = \langle v_p\rangle \xi$, $\langle v_p\rangle = \langle V_p\rangle / V_0$, and γ_0 is found by solving the ordinary differential problem

$$\frac{d\gamma_0}{d\Theta} = \mathrm{B}(\gamma_0), \tag{33}$$

$$\Theta = 0,\ \gamma_0 = 0, \tag{34}$$

where $\Theta = s\beta_0 \theta$.

If the integral in Eq. (31) cannot be evaluated analytically, Eq. (31) can be differentiated to yield

$$\frac{1}{\mathrm{B}(\gamma)}\frac{d^2\gamma}{dX^2} - \frac{1}{\mathrm{B}(\gamma)^2}\frac{d\mathrm{B}}{d\gamma}\left(\frac{d\gamma}{dX}\right)^2 + \left(N_\beta - \frac{\xi_{av}}{\mathrm{B}(\gamma)}\right)\frac{d\gamma}{dX} = 0, \tag{35}$$

where in addition to the boundary condition (32) we have

$$X = 0,\ \frac{d\gamma}{dX} = -\mathrm{B}(\gamma_0)\left(N_\beta \gamma_0 - \xi_{av} \int_0^{\gamma_0} \frac{d\gamma}{\mathrm{B}(\gamma)} \right). \tag{36}$$

When the function Γ is determined from Eqs. (32)–(36), the integral equation (23) can be solved by the method of successive approximations at three points, and then the function $\langle v_p\rangle$ can be built for the whole time interval using the interpolating function

$$v_{av} = \left(1 + a_1 \tau^{a_2}\right)^{-a_3}, \tag{37}$$

where a_1, a_2, a_3 are positive constants determined using the three known values of v_{av} and corresponding time intervals.

Figs. 2-3 illustrate the dependence of the dimensionless permeate flow rate and filtrate concentration on time calculated by the numerical and end-point interpolation methods. As in [1] with reversible adsorption, the adsorber with irreversible adsorption can provide a constant production rate at constant TMP for a sufficiently long separation cycle. It is also seen that the approximate method with a computation time of few minutes provides a practically acceptable error in calculating the desired curves. Thus, the

approximate method can be used in engineering calculations instead of the high-accuracy numerical method, which requires many hours of computation time.

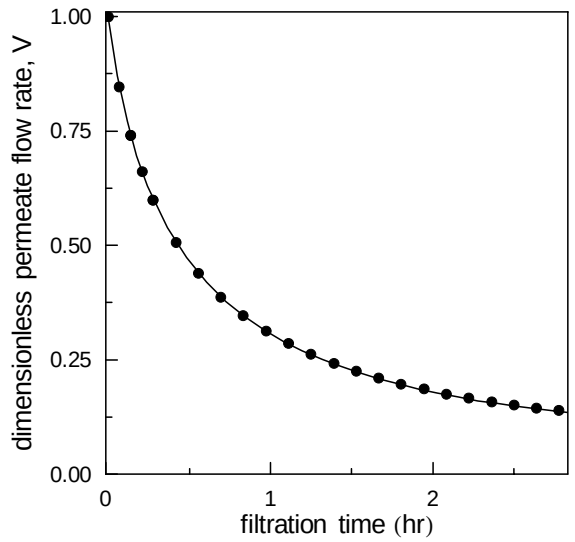

Fig. 2. Decline of permeate flow rate with time ($N_\beta = 2.25$, $N_\chi = 0.01$, $\xi = 1$, $s\beta_0 = 0.18\ \mathrm{s}^{-1}$, $\mathrm{B}[\gamma] = 1 - 8.3\times10^{-4}\,\gamma$): line – approximate solution, circles – numerical solution.

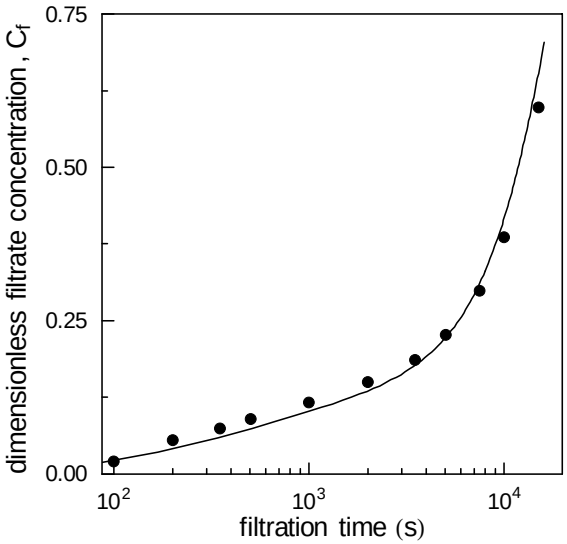

Fig. 3. Variation of filtrate concentration with time ($N_\beta = 2.25$, $N_\chi = 0.01$, $\xi = 1$, $s\beta_0 = 0.18\ \mathrm{s}^{-1}$, $\mathrm{B}[\gamma] = 1 - 8.3\times10^{-4}\,\gamma$): line – approximate solution, circles – numerical solution.

1. Yu.S. Polyakov, Membrane Quarterly, 2005, Vol. 20, No. 3.
2. C. Tien, Granular Filtration of Aerosols and Hydrosols, Butterworths Publishers, Boston, USA, 1989.
3. Yu.S. Polyakov, Theoretical Foundations of Chemical Engineering, 2005, Vol. 39, No. 5.
4. Yu.S. Polyakov, Dilman V.V., Approximate method … Herein (В настоящем сборнике).